A Study on Centrifugal Pump Performance treating Different Fluids

R.S. Afify[1*], N.H. Abdou[2], M.H. Salem[3] and K.A. Ibrahim[4]

[1] Mechanical Engineering Department, College of Engineering and Technology, Arab Academy for Science, Technology and Maritime Transport (AASTMT), Abu kir, Alexandria, P.O.Box1029-Miami, Egypt. Tel.: +201030576111, rola@aast.edu.
[2] Mechanical Engineering Department, College of Engineering and Technology, Arab Academy for Science, Technology and Maritime Transport (AASTMT), Abu kir, Alexandria, P.O.Box1029-Miami, Egypt. Tel.: +20 12 77677005, nour.nasser232@gmail.com
[3] Mechanical Engineering Department, College of Engineering and Technology, Arab Academy for Science, Technology and Maritime Transport (AASTMT), Abu kir, Alexandria, P.O.Box1029-Miami, Egypt. Tel.: +20 10 03349888, mahmoudhsalem@aast.edu
[4] Mechanical Engineering Department, Faculty of Engineering, Menofia University, Menofia, Egypt. Tel.: +201003339503, kamalabd49@gmail.com
[*] Corresponding Author: AASTMT, Abu kir, Alexandria, P.O.Box1029-Miami, Egypt. Tel.: +201030576111, rola@aast.edu.

Abstract

Understanding centrifugal pump local flow characteristics under different piping systems flow conditions is important. Single and two-phase flows applications via centrifugal pump are widely used in many industries. In the present work, the behavior of emulsion (oil-in-water) and air-water mixture flows through a single stage radial flow type centrifugal pump at three different pump rotation speeds has been studied experimentally and analytically. Effects of oil type, oil concentrations and air injected into the pump suction side on the pump performance under different operating conditions were considered. For each operating condition, pump discharge, generated head, efficiency and the power required to drive the pump were mainly affected by the type of oil, oil concentrations, the amount of air bubbles flowing through the pump impeller and the air injection position in the suction pipe. The results obtained from this study are valuable for chemical and petroleum industries.

Keywords: Pump performance; Analytical; Experimental; two phase flow; Emulsion flow.

Nomenclature

A	Area, cross section (m^2)
a	Distance between vanes (m)
A_c	Volute throat area (m^2)
b	Width of vane (m)
c	Absolute velocity (m/s)
C	Coefficient
$C_{fr,La}$	The impeller friction loss coefficient
C_{sh}	The shock loss coefficient (0.5 – 0.7)
c_{1u}	The circumferential components of absolute velocity at inlet (m/s)
c_{2u}	The circumferential components of absolute velocity at outlet (m/s)
c_{ax}	Axial velocity in gap
d	Diameter (m)
e	The blade thickness
g	Gravitational acceleration
H	Head
k	Rotation factor
k_w	Influence of impeller inlet diameter on slip factor
l	Length
L	Air entry distance from pump (m)
le	The blade length (m)
$L_{sh,La}$	Impeller loss (m)
n	Rotational speed (revolutions per minute)
p	Pressure
P	Power
P_{me}	The mechanical power loss due to the bearing and axial thrust losses (1% of the useful power)
Q	Flowrate
Q_h	Flowrate through auxiliaries (zero)
Q_i	The impeller flow (m^3/s)
Q_{La}	Pump flow (m^3/s)
Q_{sp}	Pump internal leakage flow (m^3/s)
r	Radius
Re	Reynolds number
s	Gap width
s_{ax}	Axial distance between impeller shrouds and casing
u_1	Circumferential velocities (m/s)
u_2	Circumferential velocities (m/s)
w	Relative velocity
y	Geometry
z	Number of blade
Z	Sum of hydraulic losses
α	Angle between direction of circumferential and absolute velocity
β	Angle between relative velocity vector and the negative direction of circumferential velocity
γ	Slip factor

δ	Deviation angle
ε	Roughness
η	Efficiency
ν	Kinematic viscosity
ξ_{EA}	Inlet + outlet loss
ρ	Density
τ	Blade blockage factor
λ	Friction coefficient

Subscripts

1	Impeller blade leading edge
2	Impeller blade trailing edge
av	Average
ax	Axial
c	Casing/volute
e	Blade or vane
fr	Friction
h	Hydraulic
inf	Infinity
La	Impeller
m	Mechanical component
me	Mechanical
n	Inner diameter of suction nozzle
p	Static pressure created by impeller
q	Average velocity calculated from continuity (to be distinguished from velocity vector)
r	Real
s	Shaft
sh	Shock
sp	Annular seal, leakage flow
th	Theoretical
u	Circumferential component
v	Volumetric

1. Introduction

The performance characteristics of a centrifugal pump for moving pure water are principally known. Functioning centrifugal pumps with gas and fluids may lead to a degradation of their performance. The effect of moving air or oil or both of them besides water by a centrifugal pump is under considerations.

Considering local characteristics of two-phase flow for different flow conditions in piping systems is important for industrial process design and optimization for higher productivity and lower cost. Starting with two-phase flow (Liquid / gas), **Liu et al. [1]** conducted experimentally air-water two-phase flow in a horizontal pipe. They exposed the structural features of each phase. Also, they three-dimensionally presented transient flow fluctuation energy evolution and characteristic scale distribution. **Zeghloul et al. [2]** presented the findings obtained from two-phase flowrate measurements using venturi meters. **Shao et al. [3]** experimentally and numerically studied two-phase flow patterns and the flow characteristics in transparent centrifugal pump suction chamber. **Song et al. [4]** numerically simulated centrifugal pump performance using two-phase flow method. Cavitation effects look like entrained air, **Ma and Liu [5]** numerically discussed the cavitation characteristics for centrifugal pumps.

Following with two-phase flow (liquid / liquid), horizontal segregated two-phase flows (oil-water) are usually existed in oil wells. The pressure drop is a significant parameter to estimate the horizontal oil well productivity. **Zhaia et al. [6]** introduced dynamic contact angle by solving Young-Laplace equation to compute the oil-water interface shape. Inside a centrifugal pump impeller, **Perissinottoa et al. [7]** experimentally investigated the behavior of water drops in an oil medium. In the same manner, t**hey [8]** investigated the behavior of oil drops in a water medium. They carried out their experiments for different water flowrates and pump speeds. They also captured the flow patterns using high-speed camera. Moreover within a centrifugal pump impeller, **Rafael [9]** used image processing and deep-learning approaches to follow and process the mobility of oil droplets in a two-phase oil-water flow. In a transparent impeller, **Chang et al [10]** detected gas-liquid flow for three-phase centrifugal pump performance according to air volume.

Two-phase flow (liquid / liquid) may be considered as a one-phase flow if they were mixed well and this was called emulsion flow. For curved diffusers, **El-Askary et al. [11]** presented an experimental study on emulsion flow. **Mandal and Bera [12]** experimentally studied the variation of the rate of flow of oil-in-water emulsions with pressure drop and they calculated rheological parameters. The pressure drop increased as oil concentration in the oil-in-water emulsion increased due to high viscosity.

Nädler and Mewes [13] investigated experimentally the two immiscible liquids flow and the influence of an additional inserted gas phase in transparent horizontal pipes. The pressure drop of the three phase flow system was of the magnitude as the pressure drop of the two phase flow of gas and the dominating liquid phase. However, **Saushin and Goltsman [14]** numerically simulated air-water-oil mixture flow in a horizontal pipe. They revealed the developed stable flow regimes. They concluded that, in real oil production conditions, it is not recommended to use the isokinetic probes of the flow in front of the sampling section without preliminary preparation. Moreover, **Ren et al. [15]** conducted a series of experiments to examine the transitions flow pattern and water holdup taking into consideration both vertical and horizontal sections of a transportation pipe. For the same flow, **Hanafizadeh et al. [16]**

used a qualified digital camera to experimentally investigate air-water-oil three-phase flow pattern in an inclined pipe. Besides, **Spedding et al. [17]** presented holdup data were accessible in a horizontal pipe for three-phase co-current oil-water-air. They confirmed the validity of the employed experimental technique by detailed two-phase studies.

Ma et al. [18] combined a blind tee, a Venturi meter, and a gamma-ray densitometer to develop a method for flowrate measurement in horizontal three-phase flows of oil-gas-water. Moreover, **Doherty et al. [19]** investigated the three-phase air/oil/water horizontal flow in a symmetrical impacting tee junction. Their observed flow regimes agreed with an existing three-phase flow map. **Ibrahim and El-Kadi [20]** experimentally tested the behavior of a centrifugal pump pushing air-water-oil flow. Also, **Ganat et al. [21]** experimentally studied the influence of gas injection on the phase inversion in oil-water flows through vertical transparent pipe. **Wang et al. [22]** numerically studied the electrokinetic motion of a charged oil droplet near a charged air-water interface. **They [23]** also interpreted the logging information of three-phase oil-air-water flow patterns using a new method in small-diameter vertical measurement channels. **Sun et al. [24]** used vortex flowmeter to experimentally measure the oil-gas-water three-phase flow due to its several characteristics.

For three-phase flow (liquid / solid / gas), the ratio of the permeability of soil to air and to water is an index of stability of soil structure. **Reeve [25]** measured first the permeability of a soil using water and air. They used entrapped air as a measuring fluid to study the effect of water contained in the soil on permeability.

A lot of applications are related to Multi-phase flows. **Steimes et al. [26]** mentioned that lubrication system of aero-engines in air-sealed bearing chambers managed a two-phase oil-air flow. **Donga et al. [27]** investigated cost reduction technology for high water cut oil producing well problem. **Xu et al [28]** presented a variable hysteresis control algorithm for air-to-water heat pump (AWHP) supply water temperature. **Steimes et al [29]** summarized the outcomes of an air-oil prototype of extracting a specific phase from a multiphase flow. Moreover, **Ganat [30]** reviewed the types and applications of pumping systems. **Kaluarachchi and Parker [31]** described computationally a simple procedure for modeling the effects of entrapped oil on permeability-saturation-capillary pressure relations. The objective of **Perissinotto et al. [32]**'s work was to examine how an oil-water emulsion forms in the transparent impeller and volute of a prototype electrical submersible pump (ESP). Images showing the behavior of oil droplets injected into water at various flow rates and rotation speeds were produced by flow visualization techniques. "Concentrated drops" and "dispersed drops" are the two patterns that are found. **Zhao et al. [33]** studied the effect of centrifugal pump rotation speed, liquid flow rate and inlet gas volume ratio on pump flow patterns. They recognized four common flow patterns; segregated flow, bubble flow, gas pocket flow, and aggregation bubble flow.

The main objectives of the present work are studying pump performance characteristics at these cases: -

1. Water and oil (emulsion) with different concentrations.
2. Water and oil (emulsion) with two different oil densities.
3. Water and air injected at different stations along the suction line and with different flow rates.

2. Analytical Analysis

The fundamental equation (without swirl) of turbo-machines with infinite blade is declared by Euler [34] as:

$$H_{\inf} = \frac{\left(u_c c_{2u} - u_1 c_{1u}\right)}{g} \tag{1}$$

After introducing the slip factor γ and the blade blockage τ_2, the theoretical head will be [35]:

$$H_{th} = \frac{u_2^2}{g}\left(\gamma - \frac{Q_{La}}{A_2 u_2 \tan\left(\beta_{2B}\right)}\left[\tau_2 + \frac{A_2 d_{1m}^{*} \tan\left(\beta_{2B}\right)}{A_1 \tan\left(\alpha_1\right)}\right]\right) \tag{2}$$

$$A_1 = \frac{\pi}{4}\left(d_1^2 - d_n^2\right) \tag{3}$$

$$A_2 = \pi d_{2b} b_2 \tag{4}$$

Pump performance may be evaluated using an accurate loss correlation analysis inside the pump. In the present study, the following internal losses are taken into consideration from [36]:

2.1. Leakage loss

Leakage loss happens because of smaller circulation through gaps between pump's rotating and fixed parts. Leakage loss results in a reduction in efficiency because the flow in the impeller is increased compared to the flow through the pump. To compute the leakage loss, the pressure difference over the seal at the impeller inlet ΔH_{sp} has to be recognized [35]:

$$\Delta H_{SP} = H_P - k^2 \frac{u_2^2}{2g}\left(1 - \frac{d_{sp}^2}{d_2^2}\right) \tag{5}$$

Where

$$H_P = \frac{u_2^2 - u_1^2 + w_1^2 - w_2^2}{2g} - Z_{La} \quad (6)$$

$$k = 0.9 y_{sp}^{0.087} \quad (7)$$

$$y_{sp} = Re_{u_2}^{0.3} \frac{s d_{sp}}{d_2^2} \sqrt{\frac{s}{l_{sp}}} \quad (8)$$

$$Re_{u_2} = \frac{u_2 r_2}{\nu} \quad (9)$$

$$c_{ax} = \sqrt{\frac{2g\Delta H_{SP}}{\xi_{EA} + \lambda \frac{l_{sp}}{2s}}} \quad (10)$$

The friction coefficient is calculated as:
For laminar flow *Resp* < 2300

$$\lambda = \frac{64}{\mathrm{Re}_{sp}} \quad (11)$$

For turbulent flow 4000 < Re_{sp} <10^8:

$$\lambda_0 = \frac{0.31}{\left(\log\left[A + \frac{6.5}{\mathrm{Re}_{sp}}\right]\right)^2} \quad (12)$$

As

$$\mathrm{Re}_{sp} = \frac{2 s c_{ax}}{\nu} \quad (13)$$

The effect of the rotation in turbulent flow is covered by an experimentally determined factor $\frac{\lambda}{\lambda_0}$, [35]:

$$\frac{\lambda}{\lambda_0} = \left[1 + 0.19\left(\frac{\mathrm{Re}_{u_2}}{\mathrm{Re}_{sp}}\right)^2\right]^{0.375} \quad (14)$$

The friction coefficient is calculated iteratively [35].
Subsequently, the leakage flow is calculated as follows:

$$Q_{sp} = \pi d_{sp}\, s\, c_{ax} \quad (15)$$

2.2. Impeller loss,

$$L_{sh,La} = C_{sh} \frac{\left(w_1 - w_{1q}\right)^2}{2g} \quad (16)$$

$$d_{h,La} = \frac{2\left(a_2 b_2 + A_{q1}\right)}{a_1 + b_1 + a_2 + b_2} \quad (17)$$

$$l_e = \frac{r_2 - r_1}{\cos\left(\beta_{2B}\right)} \quad (18)$$

$$L_{fr,La} = 4 C_{fr,La} \frac{l_e}{d_{h,La}} \frac{w_{av}^2}{2g} \quad (19)$$

$$\mathrm{Re}_{La} = \frac{w_{av} l_e}{\nu} \quad (20)$$

$$L_{D,La} = 0.25 \frac{w_1^2}{2g} \quad (21)$$

2.3. Efficiencies and Power

The volumetric efficiency is the ratio of pump to impeller flow:

$$\eta_v = \frac{Q_{La}}{Q_i} = \frac{Q_{La}}{Q_{La} + Q_{sp}} \quad (22)$$

Impeller flow can be considered as:

$$\varepsilon_1 = \left(\frac{Z_{La}}{\pi}\right)\left(\left(\frac{e_1}{\sin\left(\beta_{1B}\right)}\right) / d_1\right) \quad (23)$$

$$\varepsilon_2 = \left(\frac{Z_{La}}{\pi}\right)\left(\left(\frac{e_2}{\sin\left(\beta_{2B}\right)}\right) / d_2\right) \quad (24)$$

$$Q_i = c_{2m} \pi d_2 b_2 \varepsilon_2 = c_{1m} \pi d_1 b_1 \varepsilon_1 \quad (25)$$

The mechanical efficiency is given as:

$$\eta_{me} = 1 / \left(1 + \frac{\eta_h \eta_v \left(p_{me} + p_{RR}\right)}{\rho g H_{th} Q_{La}}\right) \quad (26)$$

The full equation of hydraulic efficiency is calculated from power balance of a measured pump and is given by:

$$\eta_h = \frac{\rho g H_r \left(Q_{La} + Q_{sp}\right)}{\left(p - p_{me} - p_{RR}\right)} \quad (27)$$

The actual head H_r is given as:

$$H_r = H_{th} - \left(L_{sh,La} + L_{fr,La} + L_{D,La}\right) \quad (28)$$

The overall power balance of a pump is given by:

$$P = \frac{\rho g H_r Q}{\eta_h \eta_v} + P_{me} + p_{RR} \quad (29)$$

The overall efficiency is given as:

$$\eta = \eta_v \eta_h \eta_{me} \quad (30)$$

3. Experimental Analysis

The general arrangement of the experimental apparatus is shown in Fig.1. In this study, a single stage, radial type centrifugal pump, driven by 1 hp

electric motor with a maximum rotational speed of 1650 rpm, is used. This pump was operated in a closed system consisting of suction and delivery tanks through pipelines. The centrifugal pump was equipped with facilities for measuring the pump discharge, air flow rate, suction head, delivery head, pump speed and the power required to drive the pump. The suction and delivery pressures were measured using pressure transducers. The mixture of oil and water discharge was measured by a calibrating collecting tank and a stop watch. Air flow rate was measured using a standard air rotameter.

4. Results

To forecast the performance of a centrifugal pump, two analyses are considered. The equations mentioned in the analytical analysis are considered. All the internal and external pump losses are calculated using Microsoft Excel. Moreover, in the experimental analysis suction pressure and delivery pressure are measured then manometric head is captured. Flowrate is also valued by dividing the collected volume by time. Pump performance curves (head-flowrate, efficiency-flowrate and shaft Power-flowrate curves) are presented. Finally, the actual head, power and efficiency of the pump are estimated analytically and experimentally.

4.1. Pure water flow results

Fig. 2 (a), (b), and (c) shows a comparison between analytical and experimental results of head, efficiency and shaft power, respectively, and flowrate for pure water at 1535 rpm. Fig. 2 (a) shows the measured pump head for pure water compared with the analytical results. It can be recognized from figure that the both curves have the same trend with acceptable agreement. The variation of the overall efficiency with flow rate is shown in Fig. 2 (b). The comparison between the measured and analytical results shows an acceptable agreement. Fig. 2 (c) shows the variation of pump shaft power with the flow rate. The measured results were compared with those obtained analytically at 1535 rpm impeller speed.

4.2. Water and oil (emulsion) with three concentrations (0.005, 0.01 and 0.02) Oil density of 878 kg/m^3

Fig. 3 (a), (b), and (c) shows analytical relations between head, efficiency and shaft power, respectively, and flowrate for pure water and oil of density of 878 kg/m^3 of different concentrations at 1535 rpm. From the graph, there is a very low noticeable change due to the concentration change. When zooming on graph, pure water has the maximum head descending with concentration of 0.005, 0.01 and 0.02. The reason is that an increase in oil concentration leads to an increase in friction losses.

Fig. 4 (a), (b), and (c) shows experimental relations between head, efficiency and shaft power, respectively, and flowrate for pure water and oil of density of 878 kg/m^3 of different concentrations at 1535 rpm. Experimentally wise, there is a noticeable change due to the concentration change. It is noteworthy that in both analytical and experimental studies the same order was followed. The results, given in Fig. 4 (a), indicate that under such emulsion fluid (oil-in-water) flow condition, the centrifugal pump becomes unable to generate the same head as produced in case of pure water flow. Therefore, the pump head degradation depends on the type of fluid flows through the pump impeller. Results in Fig. 4 (b) show that if oil concentration is increased the efficiency consequently decreases. This is due to an increase in the flow viscosity. Fig. 4 (c) indicates that the pump input power, at constant pump speed, increases by increasing the value of oil concentration in the mixture. This is due to the increasing value of the mixture viscosity.

Fig. 5 (a), (b), and (c) shows a comparison between analytical and experimental relation between head, efficiency and shaft power, respectively, and flowrate for pure water and oil density of 878 kg/m^3 with a concentration of 0.005 at 1535 rpm.

From results, it's evident that emulsion flow followed the same trend as pure water. In head-flowrate and shaft power-flowrate curves, Fig. 5 (a) and (c), the experimental values are lower than analytical values may be due to the accuracy of measuring devices and the theoretical assumptions. The curves have the same trend as those obtained for pure water.

4.3. Water and oil (emulsion) with two different oil densities (878 and 901 kg/m^3).

Fig. 6 (a), (b), and (c) shows experimental relations between head, efficiency and shaft power, respectively, and flowrate for pure water and oil of two different densities (878 and 901 kg/m^3) with a concentration of 0.005 at 1535 rpm.

The emulsion density is calculated from equation (31), [37]:

$$\rho_{emulsion} = (1 - c)\rho_{water} + c\,\rho_{oil} \qquad (31)$$

Pure water has density of 1000 kg/m^3 and emulsion densities are declared in table 1. From figure, it is obvious that as density increases, head and efficiency increase. A low density of surface patterning leads to a decrease of static friction force, while a higher density weakens this effect.

Fig. 7 (a), (b), and (c) shows experimental relations between head, efficiency and shaft power, respectively, and flowrate for pure water and oil of two different densities (878 and 901 kg/m^3) with a concentration of 0.01 at 1535 rpm. Results indicate that, at constant pump speed, the head established by the pump decreases with the flow rate increases for both oil densities. The results also indicate that

the pump shaft power and its efficiency are affected by changing oil density.
Fig. 8 (a), (b), and (c) shows experimental relations between head, efficiency and shaft power, respectively, and flowrate for pure water and oil of two different densities (878 and 901 kg/m^3) with a concentration of 0.02 at 1535 rpm. Regarding to concentrations of 0.005 and 0.01, results show the same trend.

4.4. Air-water flow results

Fig. 9 shows a real view of the transparent pipe in test rig and the position of the three stages; 1st, 2nd and 3rd stages that have L of 90, 75 and 60 cm, respectively. As L is the stage opining distance from the pump.
Fig. 10 (a), (b), and (c) shows experimental relations between head, efficiency and shaft power, respectively, and flowrate for pure water and air inserted at 1st, 2nd and 3rd stages at 1535 rpm. From figure, values of head and efficiency for pure water are the highest over the other values. As the distance of entrained air from pump increases, head and efficiency decrease.
The entrained air affects greatly on the pump performance. It decreases its head and efficiency and increases its shaft power. Therefore, entrained air has a harmful effect on the pump suction performance. Air or gas will widen in the impeller inlet, this blocks the flow of liquid through the impeller. Similar to cavitation, it causes decay in the pump discharge pressure.

4.5. Water and air from each 3rdstage for two air flowrates (0.5 (6x10^{-4} kg/min) and 1 lpm (1.2x10^{-3} kg/min)).

Fig. 11 show a real view of the ventilation through the transparent pipe at 1400 rpm piping at the 3rd stage.
Fig. 12 (a), (b), and (c) shows the relations between head, efficiency and shaft power, respectively, and flowrate for different air flowrate values (0.5 lpm (6x10^{-4} kg/min) and 1 lpm (1.2x10^{-3} kg/min)) at 1400 rpm and 3rd stage. From figure, values of head and efficiency for pure water are the highest over the other values. As air flowrate values increases, head decreases, efficiency decreases and shaft power increases.
Fig. 13 (a), (b), and (c) shows the relations between head, efficiency and shaft power, respectively, and flowrate for different air flowrate values at 1535 rpm and 3rd stage. From figure, values of head and efficiency for pure water are the highest over the other values. As the amount of entrained air increases, head and efficiency decrease.
Fig. 14 (a), (b), and (c) shows the relations between head, efficiency and shaft power, respectively, and flowrate for different air flowrate values at 1650 rpm and 3rd stage. From figure, values of head and efficiency for pure water are the highest over the other values.

5 Conclusions

In this work, the performance of a variable speed centrifugal pump is discussed analytically and experimentally for water, emulsion and experimentally for water-air flows. Pump works at three different pump rotation speeds (1400, 1535 and 1650 rpm) and eight flow rates (from 0 to 50 L/s). For each case, performance pump curves are drawn using analytical and experimental analyses. Moreover, comparison between both analyses is obtained. From results, it can be concluded that:

1. For pure water, as pump rotational speed raises, head, efficiency and shaft power raise.
2. For emulsion, three oil concentrations (0.005, 0.01, 0.02) and two oil densities (878 and 901 kg/m^3) are used. When the oil concentrations increase, head and efficiency decrease. The shaft power also affected by changing oil concentrations. Moreover, as density increases, head and efficiency increase. The centrifugal pump operating with emulsion flow becomes unable to generate the same head as that obtained in the case of pure water. The amount of oil in the mixture plays a role in head degradation process.
3. For water-air, air is injected from three stages with two flow rates (1.2x10^{-3} kg/min (1L) and 0.6x10^{-3} kg/min (0.5L)). As the distance of entrained air from pump increases, head and efficiency decrease. As the amount of entrained air increases, head and efficiency decrease regardless to pump rotational speed.

The experimental results largely followed the analytical results almost in all cases with the same trend and a reasonable agreement.

6 References

1. Liu, W., Tan, C., Dong, F., “Local characteristic of horizontal air–water two-phase flow by wire-mesh sensor”, Transactions of the Institute of Measurement and Control, vol. 40(3), pp. 746–761, 2018. https://doi.org/10.1177/0142331216665689
2. Zeghloul, A., Messilem, A., Ghendour, N., et al. “Theoretical study and experimental measurement of the gas liquid two-phase flow through a vertical Venturi meter “, Journal of Mechanical Engineering Science, vol. 235(9), pp. 1567–1584, 2021. https://doi.org/10.1177/0954406220947118
3. Shao, C., Bao, N., Wang, S., et al. “Study on the prediction method and the flow characteristics of gas-liquid two-phase flow patterns in the suction chamber”, International Journal of Numerical Methods for Heat & Fluid Flow, vol. 32 (8), pp. 2700-2718, June2022. https://doi.org/10.1108/HFF-08-2021-0588

4. Song, X., Luo Y., Wang, Z., "Numerical prediction of the influence of free surface vortex air-entrainment on pump unit performance", Ocean Engineering, vol. 256, 111503, July 2022. https://doi.org/10.1016/j.oceaneng.2022.111503
5. Ma, S., Liu, Y., "CFD analysis and prediction of centrifugal pump cavitation performance based on three-dimensional two-phase flow between impeller and worm gear", Journal of Physics: Conference Series, vol. 2441(1), 012048, March 2023. **DOI** 10.1088/1742-6596/2441/1/012048
6. Zhaia, L., Zhang, H., Jin, N., "Prediction of pressure drop for segregated oil-water flows in small diameter pipe using modified two-fluid model", Experimental Thermal and Fluid Science, vol. 114, 110078, 2020. https://doi.org/10.1016/j.expthermflusci.2020.110078
7. Perissinotto, R.M., Verde, W.M., Castro, M.S., et al. "Experimental investigation of oil drops behavior in dispersed oil-water two-phase flow within a centrifugal pump impeller", Experimental Thermal and Fluid Science, vol. 105, pp. 11–26, 2019. https://doi.org/10.1016/j.expthermflusci.2019.03.009
8. Perissinottoa, R.M.,Verde, W.M., Perlesb, C.E., et al. "Experimental analysis on the behavior of water drops dispersed in oil within a centrifugal pump impeller", Experimental Thermal and Fluid Science, vol. 112, 109969, 2020. https://doi.org/10.1016/j.expthermflusci.2019.109969
9. Cerqueira, R.F.L., Perissinotto, R.M., Verde, W.M., et al. "Development and assessment of a particle tracking velocimetry (PTV) measurement technique for the experimental investigation of oil drops behaviour in dispersed oil–water two-phase flow within a centrifugal pump impeller", International Journal of Multiphase Flow, vol. 159, 104302, February 2023. https://doi.org/10.1016/j.ijmultiphaseflow.2022.104302
10. Chang,L.,Xu,Q., Yang, C., et al. "Experimental study on gas–liquid flow patterns and bubble size in a high-speed rotating impeller of a three-stage centrifugal pump", Experimental Thermal and Fluid Science Volume 145, 110896, July 2023. https://doi.org/10.1016/j.expthermflusci.2023.110896
11. El-Askary, W. A., Ibrahim, K. A., Wahba, E., et al. "Emulsion (Oil-in-Water) Fluid Flow in Curved Diffuser", International Journal of Fluid Mechanics Research, vol. 40, no. 3, pp. 204-226, 2013. **DOI:** 10.1615/InterJFluidMechRes.v40. i3.20
12. Mandal, A., Bera, A., "Modeling of flow of oil-in-water emulsions through porous media", Springer, Petroleum Science, vol. 12, pp. 273–281, 2015. https://doi.org/10.1007/s12182-015-0025-x
13. Nädler, M., Mewes, D., "The effect of gas injection on the flow of immiscible liquids in horizontal pipes", Chemical Engineering & Technology, vol. 18(3), pp. 156-165, 1995. https://doi.org/10.1002/ceat.270180303
14. Saushin, I., Goltsman, A., "Uncertainty of isokinetic sampling of the phase composition of a gas-oil-water mixture at different regimes of a developed horizontal pipe flow", Journal of Petroleum Science and Engineering, vol. 195, 107901, 2020. https://doi.org/10.1016/j.petrol.2020.107901
15. Ren, G., Ge, D., Li, P., et al. "The Flow Pattern Transition and Water Holdup of Gas–Liquid Flow in the Horizontal and Vertical Sections of a Continuous Transportation Pipe", Water, vol. 13,2077,2021. https://doi.org/10.3390/w13152077
16. Hanafizadeh, P., Shahani, A., Ghanavati, A., et al. "Experimental investigation of air-water-oil three-phase flow patterns in inclined pipes", Experimental Thermal and Fluid Science, vol. 84,pp.286–298,2017. https://doi.org/10.1016/j.expthermflusci.2017.02.009
17. Spedding, P.L., Donnelly, G.F., Benard, E., " Three-phase oil–water–gas horizontal co-current flow part II. Holdup measurement and prediction", Asia-Pacific Journal of Chemical Engineering, vol. 2, pp. 130–136, 2007. https://doi.org/10.1002/apj.26
18. Ma, Y., Li, C., Pan, Y., et al. "A flowrate measurement method for horizontal oil-gas-water three-phase flows based on Venturi meter, blind tee, and gamma-ray attenuation", Flow Measurement and Instrumentation, vol. 80, 101965, 2021. https://doi.org/10.1016/j.flowmeasinst.2021.101965
19. Doherty, A.P., Murphy, A., Spedding, P.L., "Fluid flow in an impacting symmetrical tee junction III: three-phase air/water/oil flow ", Asia-Pac. J. Chem. Eng, vol. 4, pp. 432–436, 2009. https://doi.org/10.1002/apj.161
20. Ibrahim, K.A., El-Kadi, M.A., "Behaviour of Air-Water-Oil Mixture Flow through a Centrifugal Pump", ERJ. Engineering Research Journal, vol. 24 (4), pp 131-142, October 2001. https://doi.org/10.21608/erjm.2001.71137
21. Ganat, T., Hrairi, M., Regassa, S., "Experimental investigation of gas–oil–water phase flow in vertical pipes: influence of gas injection on the total pressure gradient", Journal of Petroleum Exploration and Production

Technology, vol. 9, 3071–3078, 2019. https://doi.org/10.1007/s13202-019-0703-0
22. Wang, C., Song, Y., Pan, X., et al. "Electrokinetic motion of a submerged oil droplet near an air–water interface", Chemical Engineering Science, vol. 192, pp. 264–272, 2018. https://doi.org/10.1016/j.ces.2018.07.039
23. Wang, Y., Li, H., Liu, X., et al. "A new method of measuring the oil–air–water three-phase flowrate", Chemical Engineering Communications, vol. 207, no. 1, pp. 1–16, 2020. https://doi.org/10.1080/00986445.2016.1246438
24. Sun, H., Zhang, J., Li, X., "Experimental Research of Vortex Street Oil–Gas–Water Three-Phase Flow Base on Wavelet", Proceedings of 2013 Chinese Intelligent Automation Conference , vol. 25, pp. 659-667, 2013. https://doi.org/10.1007/978-3-642-38460-8_73
25. Reeve, R.C., "Air-to-Water Permeability Ratio", Methods of Soil Analysis: Part 1 Physical and Mineralogical Properties, Including Statistics of Measurement and Sampling, vol. 9, 1965. https://doi.org/10.2134/agronmonogr9.1.c41
26. Steimes, J., Gruselle, F., Hendrick, P., "Study of an air-oil pump and separator solution for aero-engine lubrication systems", Proceedings of ASME Turbo Expo 2013: Turbine Technical Conference and Exposition, GT2013, San Antonio, Texas, USA, June 3-7, 2013. https://doi.org/10.1115/GT2013-94483
27. Donga, L., Xiaojun, Z., Hai'an, Z., "Experimental Study on Inlet Structure of the Rod Pump with Down-hole Oil-water Hydrocyclone", Procedia Engineering, vol. 18, pp. 369 – 374, 2011. https://doi.org/10.1016/j.proeng.2011.11.059
28. Xu, Z., Xu, C., Shao, S., et al. "Field experimental investigation on partial-load dynamic performance with variable hysteresis control of air-to-water heat pump (AWHP) system", Applied Thermal Engineering, vol. 182, 116072, 2021. https://doi.org/10.1016/j.applthermaleng.2020.116072
29. Steimes, J., Gruselle, F., Hendrick, P., "Performance Study of an air-oil pump and separator solution", Proceedings of ASME Turbo Expo 2012, GT2012, Copenhagen, Denmark, June 11-15, 2012. https://doi.org/10.1115/GT2012-68895
30. Ganat, T., "Processing of heavy crude oils – challenges and opportunities", 1st edition, pp. 47-72, London, united Kingdom, 2019. https://doi.org/10.5772/intechopen.74912
31. Kaluarachchi, J.J., Parker, J. C., "Multiphase flow with a simplified model for oil entrapment", Transport in Porous Media, vol. 7, pp. 1–14, 1992. https://doi.org/10.1007/BF00617314
32. Perissinotto, R., Lazaro de Cerqueira, R., Verde, W., et al. "Visualization of oil-water emulsion formation in a centrifugal pump stage", 51st Turbomachinery & 38th Pump Symposia (TPS 2022), Houston, Texas, 2022.
33. Zhao, L., Chang, Z., Zhang, Z., et al. "Visualization of gas-liquid flow pattern in a centrifugal pump impeller and its influence on the pump performance". Measurement: Sensors. 13. https://doi.org/10.1016/j.measen.2020.100033
34. Dixon, S. L., Hall, C., "Fluid Mechanics an", Burlington: Butterworth-Heinemann, 2013.
35. Gülich, J.F., "Centrifugal Pumps", Berlin Heidelberg: Springer. 2008. https://doi.org/10.1007/978-3-540-73695-0_11
36. Abdellah, K.O., Khaldi, A., Ladouani, A., "Prediction of centrifugal pump performance using energy loss analysis", Australian Journal of Mechanical Engineering, vol. 15, no. 3, pp. 210-221, 2017 https://doi.org/10.1080/14484846.2016.1252567
37. Kleinstreuer, C., "Two-phase flow: Theory and Applications", Taylor & Francis, ISBN: 1-59169-000-5, 2003. https://doi.org/10.1201/9780203734865

Conflict of Interest

The authors declared no potential conflicts of interest with respect to the research, authorship, and/or publication of this article.

Contributions

Conceptualization, R.A. and K.I.; methodology, R.A., N.A., M.H. and K.I.; Experimental, R.A., N.A., and M.H.; validation, R.A. and M.H.; formal analysis, R.A., N.A., M.H. and K.I.; investigation, R.A., N.A., M.H. and K.I.; Writing-Original draft preparation, R.A., N.A., M.H. and K.I.; Writing-Review and editing, R.A. and K.I.; visualization, R.A., N.A., M.H. and K.I. All authors have read and agreed to the published version of the manuscript.

List of Figures Captions

Fig.1. The test rig.

Fig.2. Comparison between analytical and experimental relation between (a) Head, (b) efficiency (c) Shaft Power and flowrate for pure water at 1535 rpm, respectively.

Fig. 3. Analytical relation between (a) Head, (b) efficiency (c) Shaft Power and flowrate for pure water and oil of density of 878 kg/m^3 with different concentrations at 1535 rpm, respectively.

Fig. 4. Experimental relation between (a) Head, (b) efficiency (c) Shaft Power and flowrate for pure water and oil of density of 878 kg/m^3 with different concentrations at 1535 rpm, respectively
Fig. 5. Comparison between analytical and experimental relation between (a) Head, (b) efficiency (c) Shaft Power and flowrate for oil of density of 878 kg/m^3 with a concentration of 0.005 at 1535 rpm, respectively.
Fig.6. Experimental relation between (a) Head, (b) efficiency (c) Shaft Power and flowrate for pure water and oil of two different densities (878 and 901 kg/m^3) with a concentration of 0.005 at 1535 rpm, respectively.
Fig. 7. Experimental relation between (a) Head, (b) efficiency (c) Shaft Power and flowrate for pure water and oil of two different densities (878 and 901 kg/m^3) with a concentration of 0.01 at 1535 rpm, respectively.
Fig. 8. Experimental relation between (a) Head, (b) efficiency (c) Shaft Power and flowrate for pure water and oil of two different densities (878 and 901 kg/m^3) with a concentration of 0.02 at 1535 rpm, respectively.
Fig. 9. The transparent pipe and the three stages.
Fig. 10. Experimental relation between (a) Head, (b) efficiency (c) Shaft Power and flowrate for pure water and 1 lpm (1.2x10^{-3} kg/min) air inserted at 1st, 2nd and 3rd stages at 1535 rpm, respectively.
Fig. 11. Real view of 3rd stage ventilation through the transparent pipe at 1400 rpm.
Fig. 12. Experimental relation between (a) Head, (b) efficiency (c) Shaft Power and flowrate for different air flowrate values at 1400 rpm and 3rd stage, respectively.
Fig. ١٣. Experimental relation between (a) Head, (b) efficiency (c) Shaft Power and flowrate for different air flowrate values at ١٥٣٥ rpm and 3rd stage, respectively.
Fig. 14. Experimental relation between (a) Head, (b) efficiency (c) Shaft Power and flowrate for different air flowrate values at 1650 rpm and 3rd stage, respectively.

List of Tables Captions

Table 1. Emulsion density for different densities and concentrations.

List of Figures

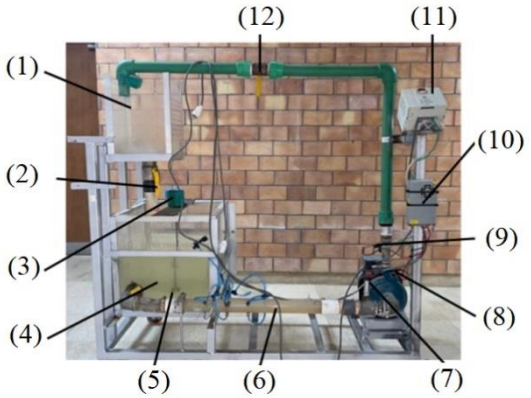

(1) Delivery tank
(2) 2nd flow control valve
(3) Mixing motor
(4) Suction tank
(5) Mixer
(6) Suction line
(7) Suction pressure transducer
(8) Pump
(9) Delivery pressure transducer
(10) Power supply
(11) Inverter
(12) 1st flow control valve

Fig.1. The test rig.

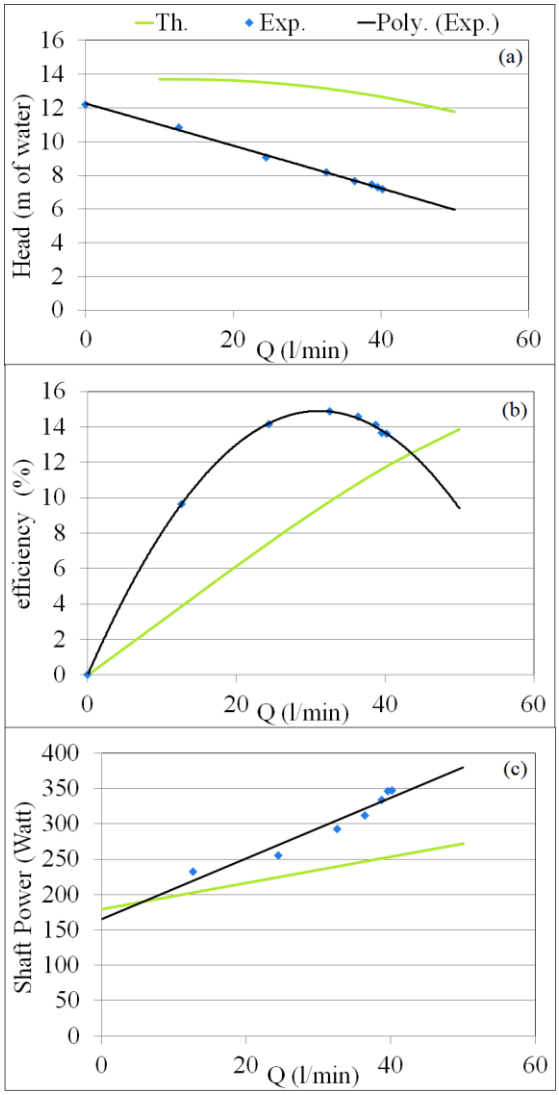

Fig.2. Comparison between analytical and experimental relation between (a) Head, (b) efficiency (c) Shaft Power and flowrate for pure water at 1535 rpm, respectively.

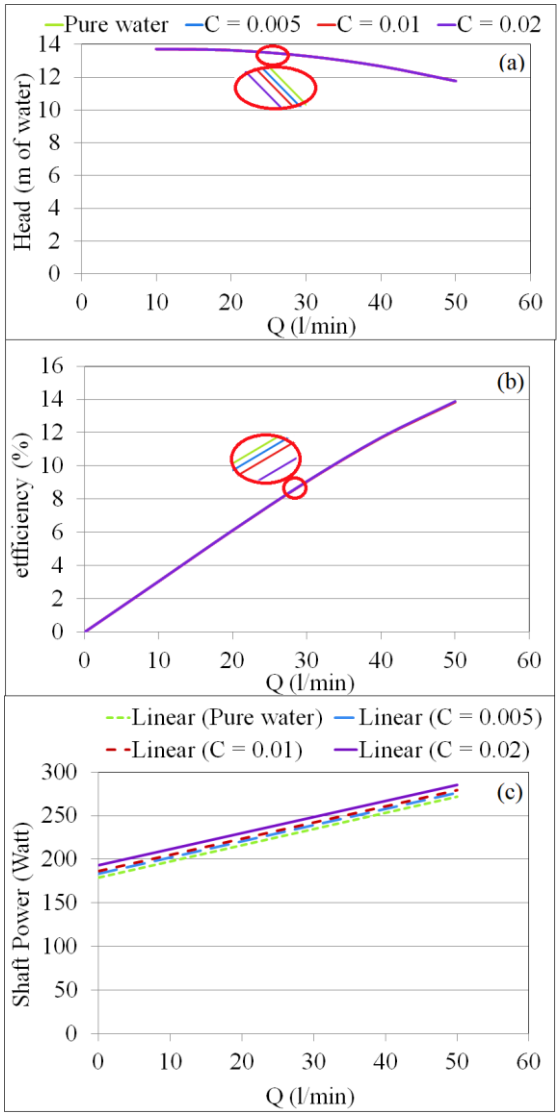

Fig. 3. Analytical relation between (a) Head, (b) efficiency (c) Shaft Power and flowrate for pure water and oil of density of 878 kg/m^3 with different concentrations at 1535 rpm, respectively.

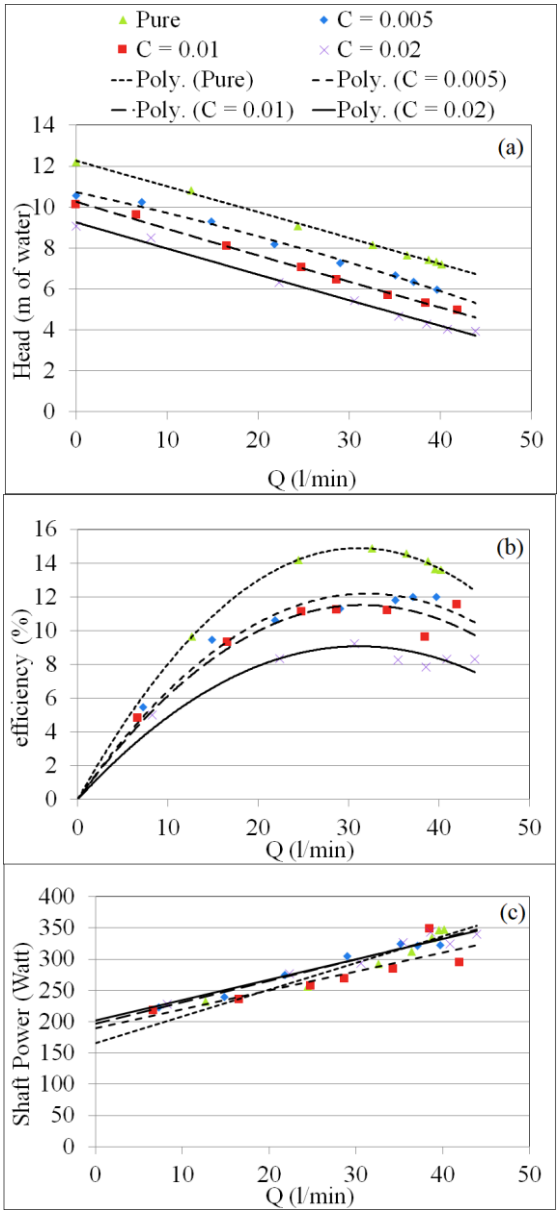

Fig. 4. Experimental relation between (a) Head, (b) efficiency (c) Shaft Power and flowrate for pure water and oil of density of 878 kg/m^3 with different concentrations at 1535 rpm, respectively.

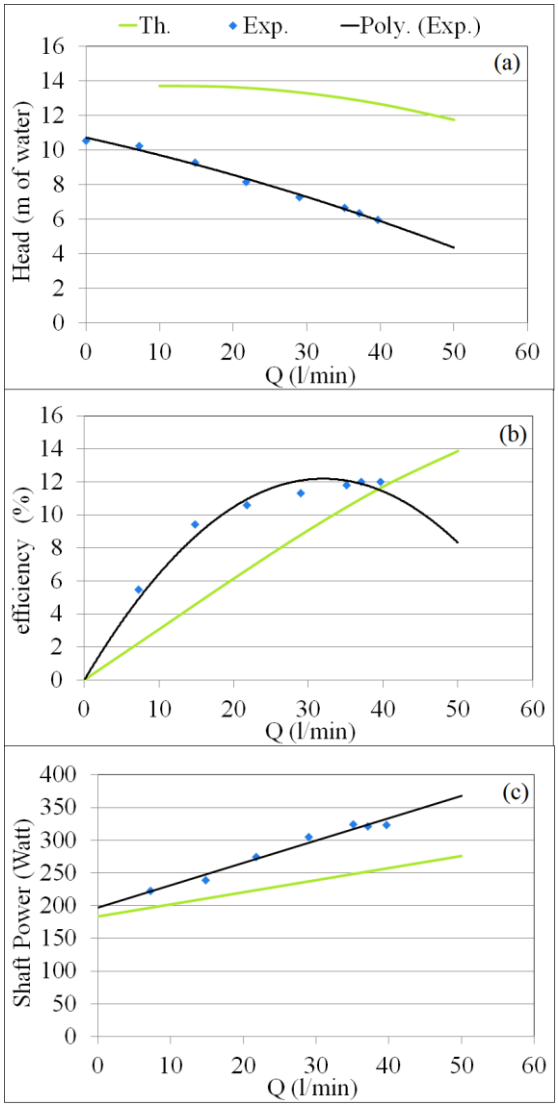

Fig. 5. Comparison between analytical and experimental relation between (a) Head, (b) efficiency (c) Shaft Power and flowrate for oil of density of 878 kg/m^3 with a concentration of 0.005 at 1535 rpm, respectively.

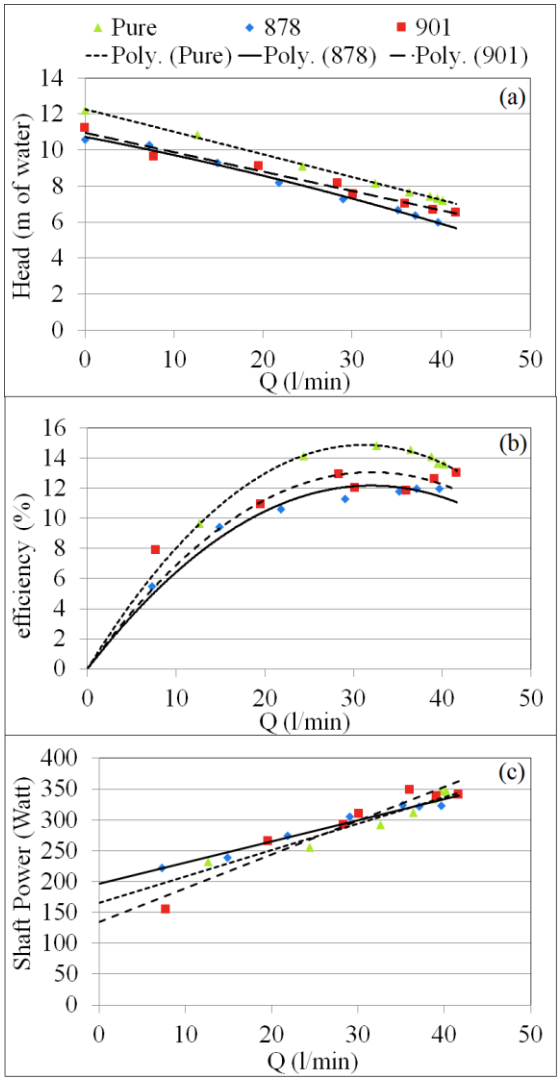

Fig.6. Experimental relation between (a) Head, (b) efficiency (c) Shaft Power and flowrate for pure water and oil of two different densities (878 and 901 kg/m^3) with a concentration of 0.005 at 1535 rpm, respectively.

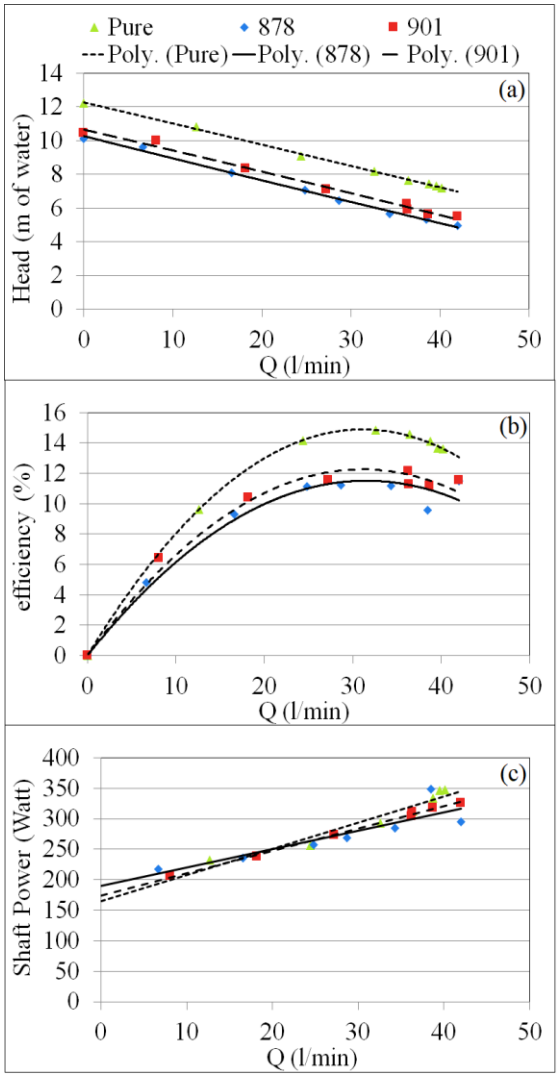

Fig. 7. Experimental relation between (a) Head, (b) efficiency (c) Shaft Power and flowrate for pure water and oil of two different densities (878 and 901 kg/m^3) with a concentration of 0.01 at 1535 rpm, respectively.

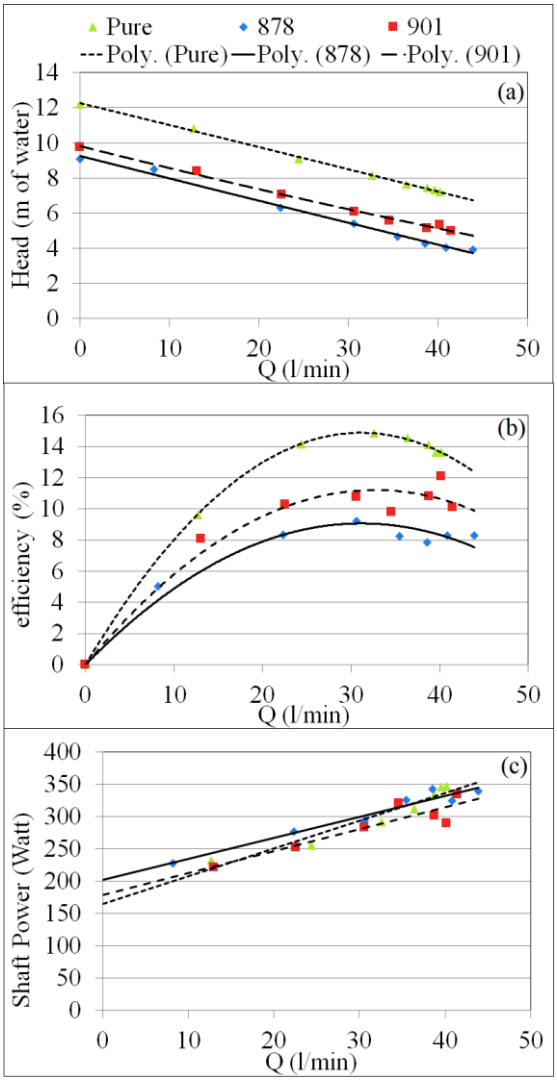

Fig. 8. Experimental relation between (a) Head, (b) efficiency (c) Shaft Power and flowrate for pure water and oil of two different densities (878 and 901 kg/m^3) with a concentration of 0.02 at 1535 rpm, respectively.

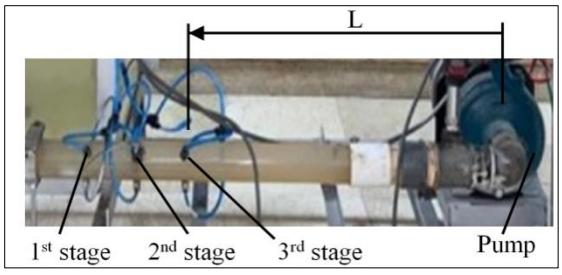

Fig. 9. The transparent pipe and the three stages.

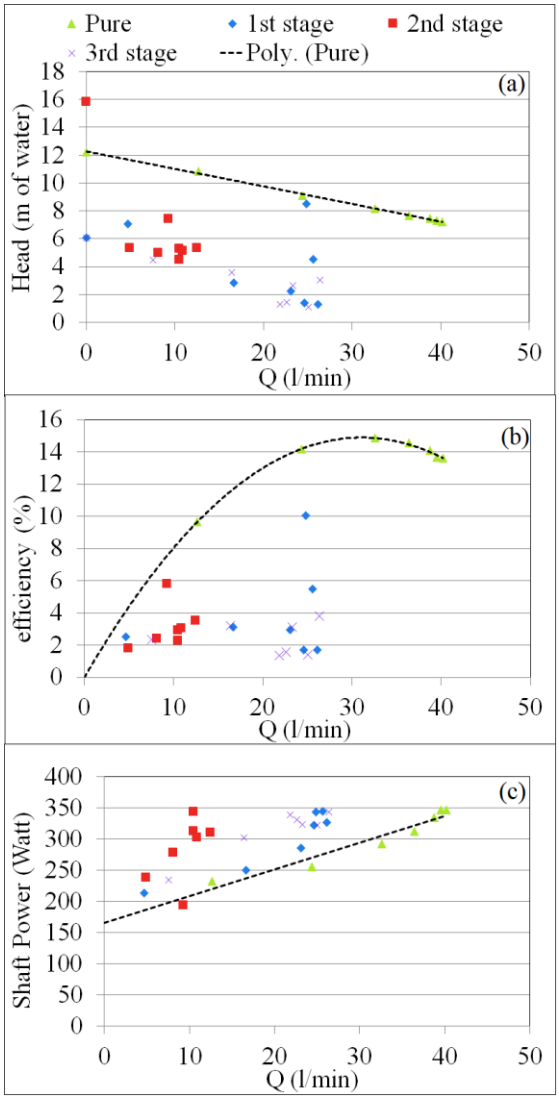

Fig. 10. Experimental relation between (a) Head, (b) efficiency (c) Shaft Power and flowrate for pure water and 1 lpm ($1.2x10^{-3}$ kg/min) air inserted at 1st, 2nd and 3rd stages at 1535 rpm, respectively.

Fig. 11. Real view of 3rd stage ventilation through the transparent pipe at 1400 rpm.

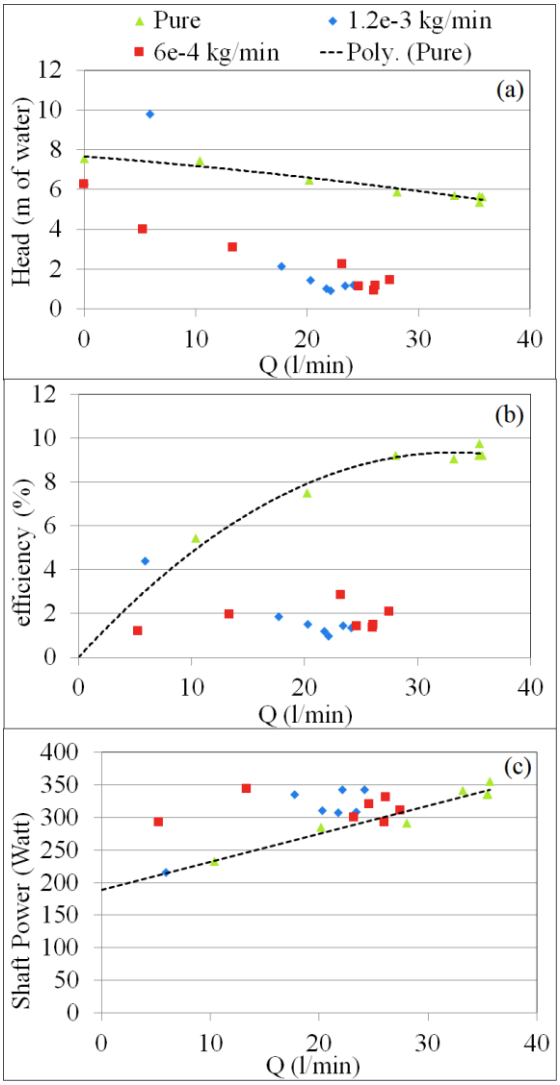

Fig. 12. Experimental relation between (a) Head, (b) efficiency (c) Shaft Power and flowrate for different air flowrate values at 1400 rpm and 3rd stage, respectively.

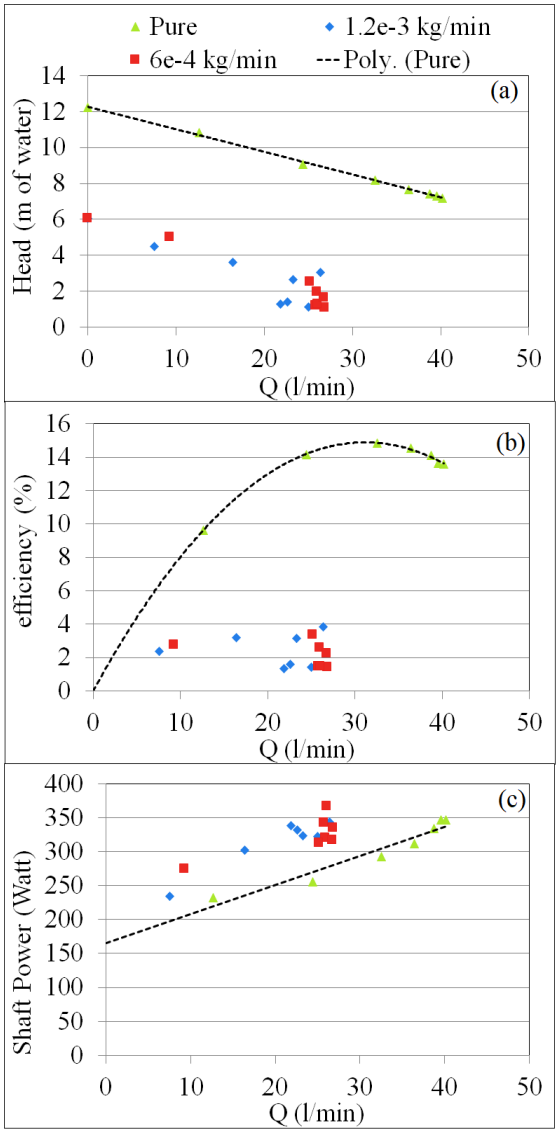

Fig. 1٣. Experimental relation between (a) Head, (b) efficiency (c) Shaft Power and flowrate for different air flowrate values at 1٥٣٥ rpm and 3rd stage, respectively.

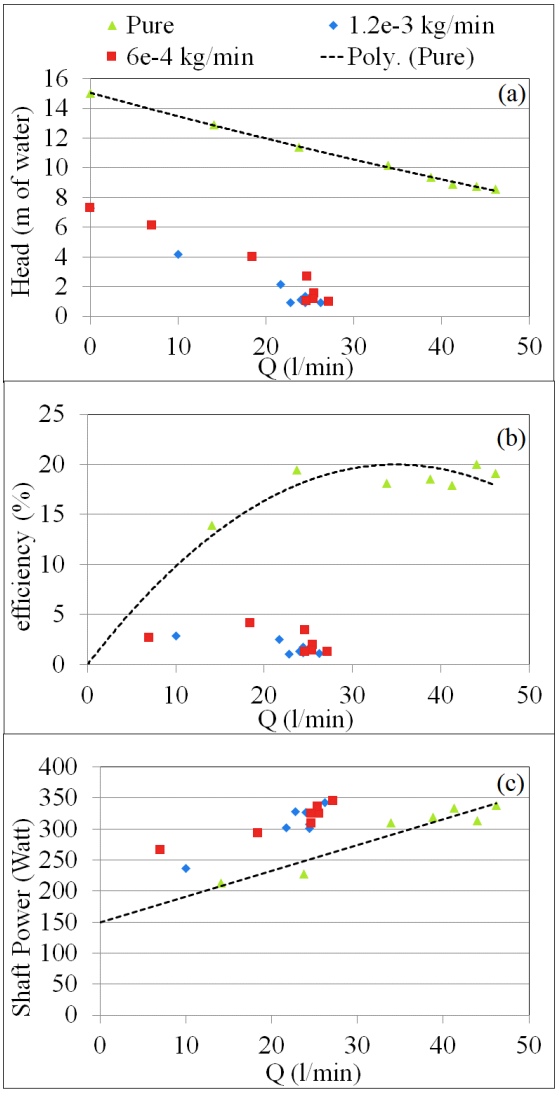

Fig. 14. Experimental relation between (a) Head, (b) efficiency (c) Shaft Power and flowrate for different air flowrate values at 1650 rpm and 3rd stage, respectively.

List of Tables

Table 1. Emulsion density for different densities and concentrations.

concentration / Density	0.005	0.01	0.02
878 kg/m^3	999.39	998.78	997.56
901 kg/m^3	999.505	999.01	998.02

Biographies

R.S. Afify is an Associate Professor at Arab Academy for Science, Technology, and Maritime Transport (AASTMT) in the College of Engineering and Technology (CET). She has academic experiences in research, teaching, supervising projects, MSc, and PhD students. Currently, her areas of research include fluid dynamics, CFD, and renewable energy.

N.H. Abdou is an MSc student at the Arab Academy for Science, Technology, and Maritime Transport (AASTMT) in the College of Engineering and Technology (CET). She has actively contributed to research, particularly through her work on a study analyzing the performance of centrifugal pumps. She is addressing practical challenges in mechanical engineering and fluid dynamics.

M.H. Salem is a Mechatronics Engineer with 15 years of experience, currently an Assistant Professor at the Arab Academy for Science, Technology, and Maritime Transport (AASTMT) in Egypt. He earned his PhD from Aston University, UK, in 2018, focusing on optimizing vibration reduction using nonlinear energy localization and genetic algorithms.

K.A. Ibrahim is a Professor at the Mechanical Engineering Department, Faculty of Engineering, Menofia University. He has academic experiences in research, teaching, supervising projects, MSc, and PhD students. Currently, his areas of research include fluid dynamics, two-phase flow, and renewable energy.